JOURNAL OF CATALYSIS **142**, 153–165 (1993)

Infrared Study of CO Oxidation over Pt–Rh/Al_2O_3 Catalysts

JAMES A. ANDERSON[1]

Department of Chemistry, The University, Dundee DD1 4HN, United Kingdom

Received September 12, 1992; revised January 4, 1993

The oxidation of CO by oxygen over two alumina-supported Pt–Rh catalysts has been studied using FTIR and an *in situ* flow reactor cell. The catalysts were tested under light-off conditions (300–573 K) over a wide range of O_2 : CO ratios (0.25–35 : 1). Invariance in the linear carbonyl stretching frequency during reaction was used as an indicator of the presence of ensembles containing only platinum atoms. Catalysts which were heated in CO at 573 K and rereduced prior to reaction showed an improvement in performance as a result of the formation of particulate rhodium at the expense of the inactive gem-dicarbonyl centres. This agglomeration of the dispersed rhodium phase was responsible for the incorporation of rhodium atoms into Pt or Pt–Rh particles. This led to the elimination of platinum only ensembles and subsequently to the formation of mixed CO/O adlayers during the reaction over catalyst prepared by coimpregnation of the metal salts. Ensembles containing only platinum atoms existed after these treatments for catalyst prepared by sequential impregnation of salts.

INTRODUCTION

Current three-way catalysts for pollutant gas emission control from automobile exhaust systems utilise both platinum and rhodium dispersed on an alumina washcoat (*1*). Platinum is the main component for CO oxidation, although rhodium is known to contribute to the overall catalysts performance especially during the warm-up period (*1*). Although the CO/O_2 reaction over the individual components has been extensively studied by infrared spectroscopy (*2–10*), less attention has been given to the bimetallic catalyst system (*11, 12*). This is surprising given reports that certain combinations of these metals may exhibit improved activity relative to the individual metals or to physical mixtures of the components (*13, 14*). There is evidence for the formation of bimetallic Pt–Rh particles in fresh and engine-aged catalysts (*13, 15, 16*) which may be influential in determining the overall catalytic activity. For example, it is known that CO oxidation over platinum occurs at the boundary between CO and O islands. As the heats of adsorption of O_2 on platinum and rhodium are significantly different, preferential adsorption of the reactant molecules may occur. If bimetallic particles contain a homogeneous mixture of Pt and Rh sites then this may result in easier mixing of the CO and O on the alloy surface with a possible faster reaction at lower temperatures (*17*). In the present paper the state of adsorbed CO and the rate of formation of CO_2 have been measured simultaneously during conditions similar to those during catalyst light-off in an attempt to relate catalytic activity of Pt–Rh/Al_2O_3 catalysts to particle morphology and arrangement of component metals on the catalyst surface.

METHODS

Platinum–rhodium catalyst [Pt–Rh(sim)] (0.5 wt% in each metal) was prepared by single-stage impregnation, which involved aqueous slurries of H_2PtCl_6 and $Rh(NO_3)_3$ with Degussa C γ-Al_2O_3. Sequentially impregnated [Pt–Rh(step)] catalyst (0.5 wt% in each metal) was prepared by a two-stage impregnation sequence, which involved addition of $Rh(NO_3)_3$ solution to a Pt/Al_2O_3 sample which had been precalcined in oxy-

---

[1] Present address; Instituto de Catalisis y Petroleoquimica, C.S.I.C., Campus de la Universidad Autonoma de Madrid, 28049 Madrid, Spain

0021-9517/93 $5.00

gen at 673 K. Samples were dried in air at 383 K and stored in vials in an evacuated desiccator until required. Catalyst samples for infrared spectroscopy were presented in the form of self-supporting discs (25 mm diameter, ca. 100 mg) formed by compressing the impregnated alumina between two polished stainless-steel dies (50 MN m^{-2}). Samples were placed in a standard glass vacuum apparatus and heated in a flow of oxygen (60 cm^3 min^{-1}) for 1 h at 673 K before evacuation at the same temperature for 15 min and then cooling to ambient temperature under dynamic vacuum. Samples were subsequently transferred to a high-temperature stainless-steel infrared cell, which also functioned as a flow reactor, and were evacuated overnight at ca. 300 K. Catalyst discs were held between two aluminium plates in which a cutaway section was positioned opposite the inlet and outlet ports thereby forcing the gases to sweep both faces of the disc before leaving the cell. Gas-phase flushing time was significantly shorter than the shortest interval used between the recording of consecutive spectra. Reduction was achieved by heating (2 h, 573 K) in a flow (150 cm^3 min^{-1}) of 3.5 vol% hydrogen in argon, and followed by evacuation at the high temperature for 15 min. Samples were then cooled to 293 K in dynamic vacuum. Hydrogen–argon was purified by passage through a commercial Deoxo unit followed by a 4A molecular sieve. Reduced catalysts were exposed to the reactant gases in a flow (50 cm^3 min^{-1}, 101 kN m^{-2}) with nitrogen making up the balance and heated in a linear temperature program ramp (10 K min^{-1}). IR spectra (4 cm^{-1} resolution, average of 4 scans, 12 s) were recorded using a Perkin–Elmer 1710 FTIR and 7500 computer.

RESULTS AND DISCUSSION

Catalyst Characterisation

Following impregnation and drying but prior to calcination and reduction, Pt–Rh(sim) and Pt–Rh(step) gave BET areas of 86 and 94 m^2 g^{-1} with average pore diameters of 30 and 28 nm with 1.7 and 4.2% microporous areas, respectively. Following calcination, Pt–Rh(sim) and Pt–Rh(step) exhibited photoelectron spectra with binding energies (eV) relative to Al $2s_{1/2}$ of 309.7 and 310.1 for Rh $3d_{5/2}$, 314.8 and 314.9 for Rh $3d_{3/2}$, and doublets at 315.8, 319.3 and 316.0, 320.0 for Pt $4d_{5/2}$, respectively. The presence of doublets for the Pt $4d_{5/2}$ signal would indicate the formation of both metal and oxide following heating in O_2 at 673 K, the presence of the former being in accordance with the thermal instability of PtO_2 under these conditions (*13*). Surface atomic ratios of Rh : Pt as determined by XPS were 2.3 : 1 for simultaneous impregnation and 2.4 : 1 for stepwise impregnation. Calcined samples, when reduced in TPR experiments, gave maxima in H_2 uptake at 373 and 413 K for Pt–Rh(sim) and at 418 and 458 K for Pt–Rh(step), while monometallic catalysts were reduced at 333 K (Rh) and at 403 and 448 K (Pt).

CO on Pt–Rh/Al_2O_3 as a Function of Temperature

In order to facilitate the interpretation of spectral features while heating in CO/O_2 mixtures, samples were treated under identical conditions in the absence of oxygen. For the sake of brevity, only spectra for the Pt–Rh(step) catalyst are shown here. Spectra for Pt–Rh(sim) were of a similar form although displaying differences in fine detail. Spectra of Pt–Rh(sim), Rh/Al_2O_3, and Pt/Al_2O_3 recorded as a function of temperature in CO have been reported elsewhere (*18*).

Spectra recorded at 303 K [Fig. 1(a)] were dominated by the twin bands at 2098 and 2029 cm^{-1} due to the rhodium gem-dicarbonyl species, $Rh(CO)_2$ (*19, 20*), with a weaker, broad maximum centered at 1854 cm^{-1} due to bridging carbonyls. Bridged carbonyl species gave maxima at 1860 (*6, 18*) and 1850 (*7, 18*) in experiments conducted under equivalent conditions for Rh/Al_2O_3 and Pt/Al_2O_3, respectively, suggest-

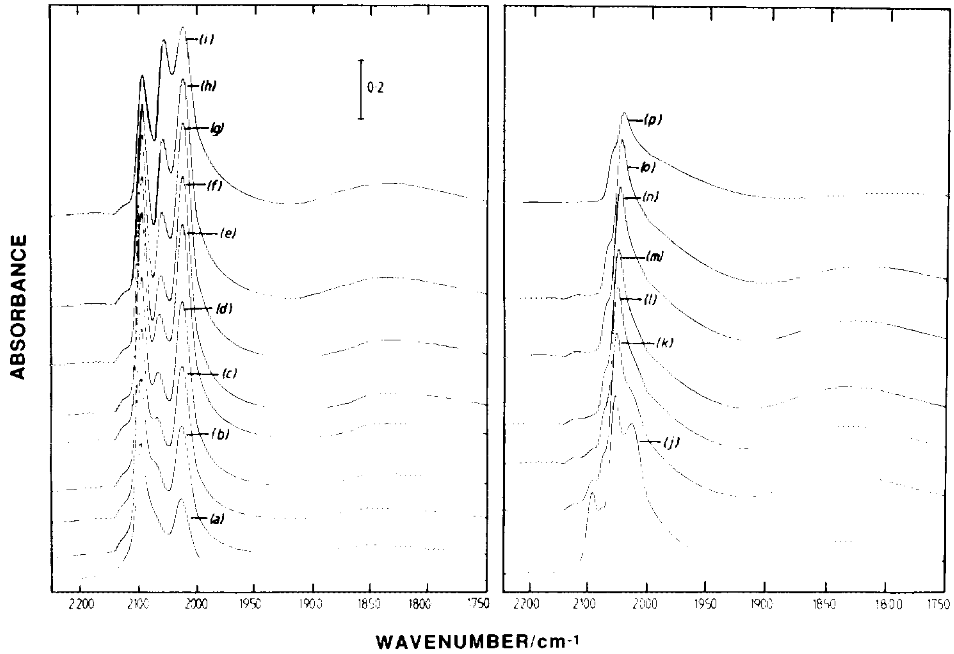

FIG. 1. Spectra of Pt–Rh(step) heated at 10 K min^{-1} in CO(1%)/N_2 recorded with the sample at (a) 303, (b) 323, (c) 348, (d) 373, (e) 398, (f) 423, (g) 448, (h) 473, (i) 498, (j) 508, (k) 518, (l) 525, (m) 530, (n) 548, and (o) 573 K. Evacuation at 573 K for (p) 1 min.

ing that neither metal gave complete coverage of the particle surfaces.

As the sample temperature was increased, the relative intensities of the pair of dicarbonyl bands changed in favour of the lower frequency component of the asymmetric stretching mode. This was accompanied by a shift of ca. 5 cm^{-1} to lower frequencies over the 300 K temperature range, consistent with previous reports (*7*, *20*). Both of these phenomena were reversed on cooling the sample in CO and are attributed to changes in coupling interactions between the carbonyls and the support and with the gas phase, the latter of which also results in a change in absorptivity (*6*) explaining the initial increases in band intensities.

Raising the sample temperature also led to the resolution of a band attributed to linearly adsorbed carbonyls, present as a shoulder at 2075 cm^{-1} with the sample at 323 K [Fig. 1(b)], and progressively shifting in frequency to give a band at 2048 cm^{-1} at 573 K [Fig. 1(o)]. The effect of heating in the presence of the gas led to an initial increase in intensity of this band, reaching a maximum in intensity in spectra of the sample at 448 K [Fig. 1(g)]. Gem-dicarbonyl bands were also initially enhanced on increasing the sample temperature, reaching a maximum intensity at 423 K [Fig. 1(f)]. These were then gradually diminished up to 498 K, although above this temperature, and in particular within the range 498–518 K, gem-dicarbonyl maxima were rapidly attenuated, and were undetectable in the IR spectra at 530 K.

The elimination of these species at elevated temperature in CO has been documented for Rh/Al_2O_3 (*18*, *21*, *22*) and Rh/SiO_2 (*23*) in the absence of platinum and may be attributed to the agglomeration of the dispersed rhodium phase and the resultant formation of particulate rhodium. This process is therefore normally accompanied by the growth in intensity of the linear carbonyl band in spectra of supported Rh (*18*, *21*, *22*), although here this effect was minimal. For example, on increasing the temperature from 498–518 K, the dicarbonyl maxima were drastically reduced without enhanced intensity of the band due to linearly bound carbonyls. However, as shown in Fig. 2, in this temperature range a dramatic shift in the band frequency occurs, which, when compared with the frequency/temperature plots for Rh alone and Pt alone, indicates that within this temperature range linearly bound Rh carbonyls begin to contribute to the spectra. Additionally, the form of the plot when compared with those of rhodium alone and a physical mixture of Pt/Al_2O_3 and Rh/Al_2O_3 (individual discs of Pt/Al_2O_3 and Rh/Al_2O_3 placed in series in the spectrometer showed an identical frequency/temperature shift to the physical mixture) would suggest that in addition to agglomeration of dicarbonyl sites to form rhodium particles, agglomeration also results in the incorporation of these atoms into existing Pt containing particles resulting in a "rhodium-like" frequency/temperature dependence of the linear carbonyl maximum. This process would be analogous to the coalescence of tiny rhodium crystallites into Rh–Pt particles on heating between 373 and 573 K in hydrogen as monitored by microscopy and XPS (*24*).

At temperatures below 508 K, the band maximum for both Pt–Rh(step) and the physical mixture of Pt/Al_2O_3 and Rh/Al_2O_3 lay below the value for Pt/Al_2O_3 but above the value for Rh/Al_2O_3 (see Fig. 8), indicating that both types of linear carbonyl species contribute to the observed maximum, again indicating that neither metal completely covers the other. The elimination of bands due to the gem-dicarbonyl species allowed the identification of an additional type of linearly adsorbed carbonyl species. This was first detected as a shoulder at 2077 cm^{-1} with the sample at 508 K, shifting to lower wavenumbers in accordance with the position of the dominant linear maximum, and finally giving a shoulder at 2069 cm^{-1} in spectra at 573 K [see Fig. 4(o)]. As argued in the case of Pt/Al_2O_3 (*6*, *8*), the higher frequency of this maximum probably indicates adsorption of CO at surfaces with more extended terraces.

A previous study distinguished between

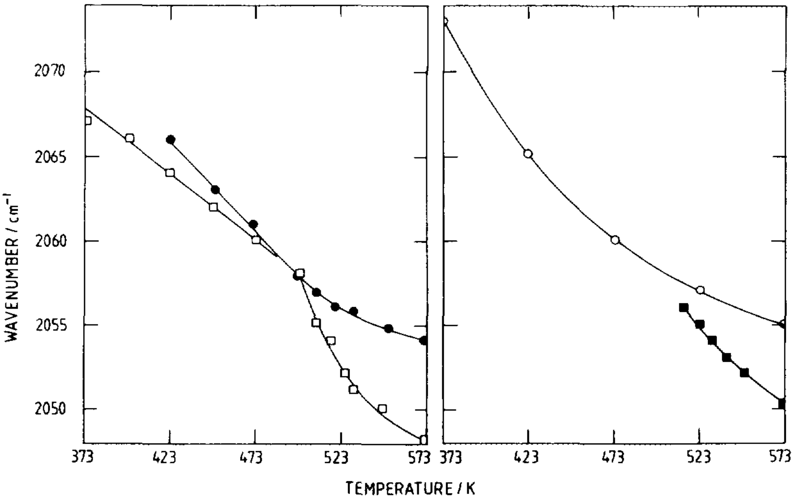

FIG. 2. Frequency (cm^{-1}) of the linear carbonyl band as a function of temperature while heating in CO(1%)/N_2 for Pt–Rh(step) (□), Pt/Al_2O_3–Rh/Al_2O_3(physical mixture) (●), Pt/Al_2O_3 (○), and Rh/Al_2O_3 (■).

the formation of linear and bridging carbonyl sites following the agglomeration of the dicarbonyl sites (*7*). The formation of sites for the former species would be consistent with the growth in both band width and intensity of the band attributed to bridging carbonyls. In addition, this maximum showed a progressive shift in frequency to lower values with a maximum at 1822 cm^{-1} at 573 K. At temperatures above 523 K, it is likely that the bridging carbonyl band represents only those species adsorbed at rhodium sites, as these carbonyls are much more weakly adsorbed on platinum (*25*) and were absent in spectra recorded above this temperature for Pt/Al_2O_3 in the absence of rhodium (*18*). These bridging carbonyls were readily removed by evacuation at 573 K [Fig. 1(p)], leaving a band at 2044 and 2062 (sh) cm^{-1} due to the linearly adsorbed carbon-monoxide.

Light-Off Temperatures as a Function of O_2 Concentration

Experiments were performed in which the inlet gas composition was maintained while increasing the temperature in a linear programmed manner. These were conducted over a wide range of O_2 concentrations (0.25–35%) and a constant CO concentration of 1%. These results are summarised in Fig. 3 for the two bimetallic catalysts and the monometallic catalysts and are shown in the form of the temperature required to obtain 50% CO conversion as a function of oxygen concentration in the gas stream. All samples show an initial improvement in performance with an increase in O_2 concentration, consistent with mechanistic studies of the reaction which indicate that at low temperatures the catalyst surface is covered with CO which acts to impede the reaction (*26*). The effect is considerably greater for Pt than for Rh at the highest CO/O_2 ratio. From kinetic modeling studies, Rh is expected to show the lower light-off temperatures (LOT) due to a combination of its higher CO desorption and surface reaction rates (*27*). Results here for O_2/CO ratios below 8 : 1 are in agreement with this expectation, and furthermore are consistent with previously reported results in which Rh exhibited the lowest light-off temperatures and where the Pt–Rh samples gave values between those of the monometallic catalysts (*28*).

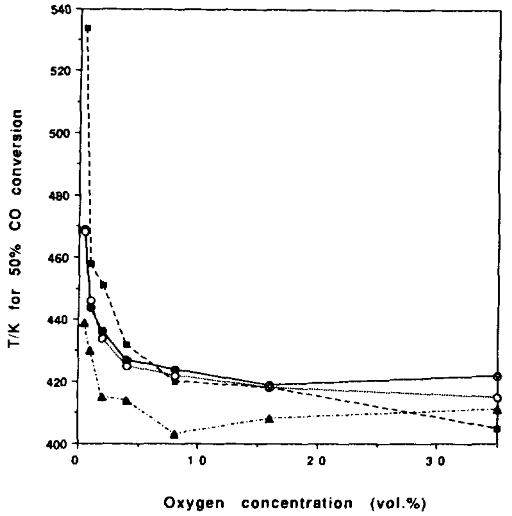

FIG. 3. Temperature required to obtain 50% CO conversion in a flow containing 1% CO as a function of oxygen concentration for Pt (■), Rh (▲), Pt–Rh(step) (○), and Pt–Rh(sim) (●).

No evidence was found for a synergistic enhancement in CO oxidation activity for the Pt–Rh catalysts relative to the monometallic components, in agreement with certain studies (*28, 29*) but in contrast to results reported by Oh and Carpenter (*14*), where only sequentially prepared samples exhibited this phenomenon. One possible explanation for the absence of this effect here and elsewhere (*28*) for sequentially impregnated samples is that deposition of one of the metal salts using acetone (*14*) is necessary. Alternatively, the presence of NO in the gas stream may have played an important role.

On increasing the O_2/CO ratio above 8 : 1, the LOT of Pt/Al_2O_3 continues to decrease while values for Rh/Al_2O_3 begin to rise above this minimum. This oxygen inhibition effect for rhodium catalysts may be attributed to the formation of the relatively inactive oxide under these extreme oxidising conditions (*7*, *14*). Plots of 80% conversion show this deactivation more dramatically due to the form of the light-off curves obtained under these conditions (*7*).

CO/O_2 on $Pt–Rh/Al_2O_3$ as a Function of Temperature

Infrared spectra obtained in a flow of CO/O_2 (1 : 16) as a function of increasing temperature are shown in Fig. 4. Spectra are shown in this example for Pt–Rh(sim), but where differences exist between the spectra of the two Pt–Rh catalysts, these will be detailed in the text. Spectra obtained under all net-oxidising conditions contained similar spectral features to those shown in Fig. 4 although the presence and intensities of band maxima at a given temperature or percentage conversion were dependent on the oxygen content of the gas stream. The four main differences between spectra obtained in a CO/O_2 flow and a flow containing CO in the absence of oxygen were as follows.

(1) Bands due to linearly adsorbed and bridge-bonded CO were eliminated. This occurred only under net-oxidising conditions and these species were eliminated at progressively decreasing temperatures as the concentration of O_2 was increased. Unlike spectra of Pt/Al_2O_3 where adsorbed CO was detected following attainment of 100% conversion of CO in the flow (*6*, *8*), spectra of $Pt–Rh/Al_2O_3$ were devoid of linear and bridged forms of adsorbed carbonyls at temperatures corresponding to complete CO conversion

(2) There was failure to eliminate completely bands due to the gem-dicarbonyl species under net-oxidising conditions. At stoichiometry or in a CO excess, these species were eliminated albeit at higher tem-

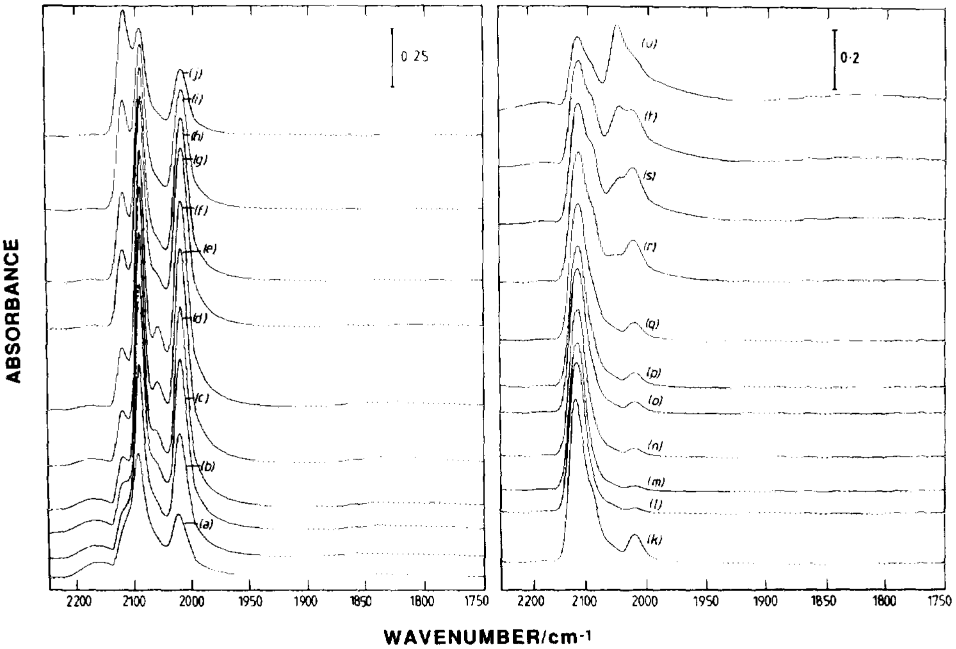

FIG. 4. Spectra of Pt–Rh(sim) heated at 10 K min^{-1} in $CO(1\%)/O_2(16\%)/N_2$ recorded with the sample at (a) 303, (b) 348, (c) 375, (d) 398, (e) 423, (f) 448, (g) 463, (h) 473, (i) 498, (j) 523, (k) 548, and (l) 573. Catalyst subsequently held at 573 K for (m) 3 min in the gas mixture and then for (n) 1, (o) 2, (p) 3, (q) 4, (r) 5, (s) 6, (t) 7, and (u) 10 min after switching off the supply of O_2.

peratures than those required while heating in the absence of oxygen.

(3) There was absence of linearly bound rhodium species generated concurrently with the diminishing intensities of the gem-dicarbonyl bands under conditions of O_2 excess. Under net-reducing or stoichiometric conditions, adsorption sites for linear carbonyl species were produced during the depletion of the dicarbonyls, although the overall contribution that this maximum made to the spectrum was less significant than while heating in the absence of O_2.

(4) A band appeared at ca. 2125 cm^{-1}. This was identified in all sets of spectra obtained under net-oxidizing conditions, but was absent for net-reducing and stoichiometric ratios. It was initially detected at progressively lower temperatures as the oxygen concentration was increased, and was of a greater relative intensity under the most extreme oxidising conditions. This band was also observed under similar conditions in spectra of Pt/Al_2O_3 (*6, 8*) and Rh/Al_2O_3 (*7*) and probably indicates adsorption of CO at sites of cationic nature. The distinction between sites of this nature on Rh or Pt would be difficult to make and the band here probably reflects adsorption at both types of ionic centre.

Following a short period during which the CO/O_2 flow was maintained at 573 K [Fig. 4 (l, m)], the O_2 supply was halted, while maintaining the flow of CO in nitrogen at the same temperature. The first spectral change observed was the growth of maxima at 2027 and 2098 (sh) cm^{-1}. As in the case of Rh/Al_2O_3 (*7*), the rapid reestablishment would indicate that a proportion of the Rh+ sites responsible for adsorption in the dicarbonyl mode remain unreduced and unagglomerated during heating in CO/O_2 and that CO desorption from these sites directly into the gas phase occurs. That is, the presence of excess oxygen in the gas stream results in CO desorption from the dicarbonyl sites rather than an agglomeration process, thereby maintaining the dispersed Rh phase. After extended periods of time, CO adsorbed in the linear mode was detected, firstly as a shoulder at 2051 cm^{-1}, and then moving to 2052 and 2057 cm^{-1} as the intensity increased [Fig. 4 (s)–(u)]. A broad band at 1820 cm^{-1} due to bridge-bonded carbonyls was also detected during this period. The relatively slower development of linear/bridged maxima compared with dicarbonyl bands on switching off the O_2 supply would suggest that removal of adsorbed oxygen was required before reestablishing adsorbed carbonyl species in the former modes. During growth of the linear maximum, bands due to the gem-dicarbonyl were gradually diminished in intensity, indicating that in the absence of oxygen, agglomeration of the sites responsible for such species was allowed to proceed. The band at 2125 cm^{-1} also diminished as a function of time in the absence of oxygen, indicating some degree of reduction of the cationic sites while heating in CO. However, in agreement with previous reports (*3, 6, 7, 11*), oxygen associated with such species was not readily removed in CO, even after extended periods of time at elevated temperatures. The possibility that such species are stabilised by the presence of residual chloride in the support, should not be discounted.

CO/O_2 on Rereduced Pt–Rh/Al_2O_3 as a Function of Temperature

Following removal of adsorbed oxygen in the manner described above, catalysts were cooled in a flow of N_2 and rereduced according to the standard reduction procedure. The resultant spectra for the sample Pt–Rh(sim) in a flow of 16% O_2/1% CO, are shown as a function of temperature in Fig. 5. As indicated by the difference in absorbance scales in Figs. 4 and 5, the rhodium gem-dicarbonyl bands were considerably attenuated during the pretreatment schedule. This would indicate that following agglomeration of the sites responsible by treatment in CO at 573 K, the disruption in CO at 300 K[21] [Fig. 5(a)] is only partially successful in redeveloping these adsorption

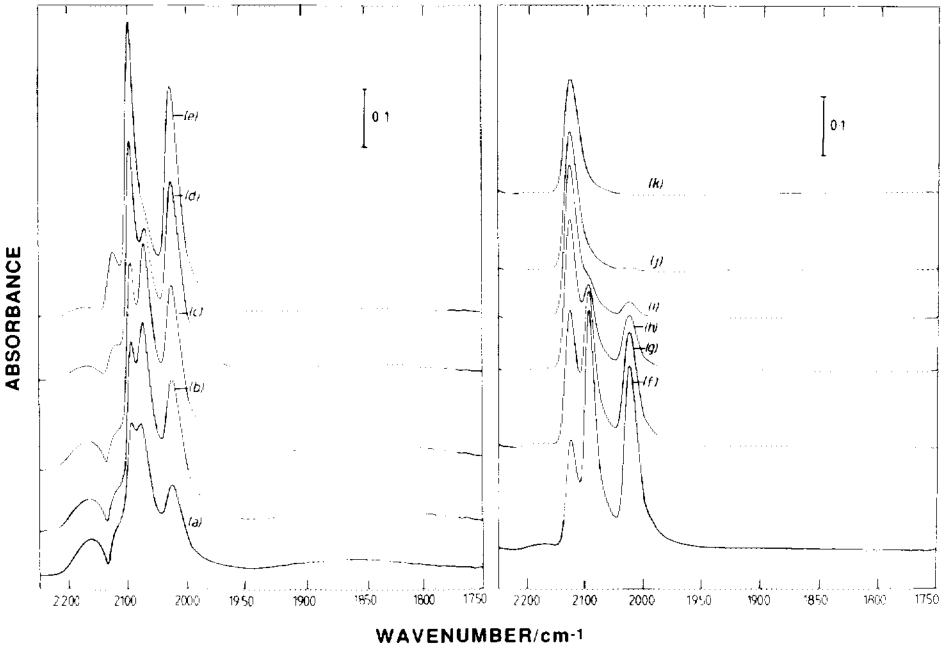

FIG. 5. Spectra of Pt–Rh(sim) for a sample previously used in Fig. 4, rereduced as described in text and heated at 10 K min^{-1} in CO(1%)/O_2(16%)/N_2 and recorded with the sample at (a) 303, (b) 348, (c) 373, (d) 398, (e) 414, (f) 448, (g) 473, (h) 498, (i) 523, (j) 548, and (k) 573 K.

centres. That is, the disruption–agglomeration process is only partially reversible. In further contrast with Fig. 4, spectra of the catalyst recorded at 300 K, clearly resolve the band due to linear carbonyl species at 2083 cm^{-1}. This band was no longer visible as a resolved maximum in spectra of the catalyst at 414 K [Fig. 5(e)], in contrast with the behaviour of this species in the fresh catalyst where a temperature of 448 K [Fig. 4(f)] was required. The elimination of bridge-bonded CO from the spectra in the same temperature range left maxima at 2024 and 2095 cm^{-1} due to the gem-dicarbonyls and at 2125 cm^{-1} due to CO at exposed sites of cationic nature, consistent with the negligible reactivity of CO at these centres. Bands due to the latter species were still dominant in spectra recorded at 573 K [Fig. 5(k)], whereas gem-dicarbonyl maxima were progressively diminished by increasing the temperature from 448 to 573 K, and were undetectable at the highest temperature. These species could be reestablished by switching off the supply of oxygen in the stream.

50% CO Conversion Temperatures for Rereduced Catalysts

The effect on catalyst performance of rereduction following reaction is summarised in Fig. 6, where the temperature for 50% CO conversion may be compared with the performance of the fresh catalysts. The 50% conversion temperatures for Pt and both Pt–Rh catalysts at 16 : 1 O_2/CO were identical for the fresh catalysts. Treatment in CO at 573 K followed by rereduction had minimal effect on the LOT of Pt/Al_2O_3 (*8*), but led to significant improvements for rhodium containing catalysts with between 20 and 30 K reduction in LOTs. This treatment was apparently more effective for Pt–Rh than rhodium alone, with the rereduced Pt–Rh(sim) catalyst almost as efficient as rhodium alone. These results for rhodium-

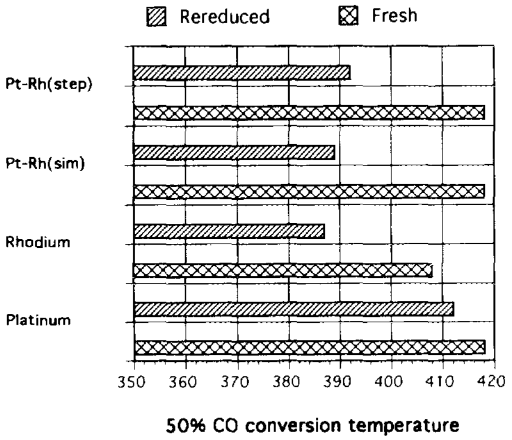

FIG. 6. Comparison of the effect of heating in CO at 573 K and then rereduction on the 50% CO conversion temperatures in CO(1%)/O$_2$(16%) for the bimetallic and monometallic catalysts.

containing catalysts are consistent with data reported by Taylor (*1*) and D'Aniello *et al.* (*28*) which show that several run-ups are required to obtain a Rh/Al$_2$O$_3$ catalyst with a stable LOT, and that considerable improvements were obtained between the first and last run-up (*28*). However, it should be emphasised that such improvements are only obtained following reaction under CO-rich conditions, or when pretreatment has included a period in which the catalyst was heated in CO alone, allowing agglomeration of rhodium to occur. When a third run-up was performed following reaction under net-oxidising conditions, and then rereduced in H$_2$, no improvement in LOT was obtained. However, if this third run-up was preceded by a treatment which included heating in CO at 573 K, further reduction in LOT occurred.

These results are consistent with those reported for Pt-Rh/CeO$_2$-Al$_2$O$_3$ in which exposure to a rich mixture during an initial run-up resulted in a subsequently reduced LOT for run-up 2, whereas exposure to a lean mixture resulted in a relatively less active catalyst in the subsequent run-up (*30*). However, Nunan *et al.* (*30*) attributed this activation in a rich mixture to the presence of hydrogen, whereas here, the reactant gas which had the most significant effect on LOT is CO. In further disagreement, Pt was thought to be the key noble metal component, which, according to the conditions during the run-up, was responsible for the most dramatic changes in subsequent LOT (*30*). Results here [Fig. 6] clearly indicate that rhodium is the more influential in dictating LOT. Studies of the alumina-supported monometallic components (*7, 8*) show that the form of the light-off curve in second and subsequent run-ups is steeper (greater change in %CO conversion within the same fixed temperature range) than for the first run-up, and this was considered as characteristic of a more "metal-like" catalyst (*32*). For Pt-Rh catalysts here [Fig. 7], gradients were equivalent in first and second run-ups despite the shift in the LOT between them. This contrasts with the form of light-off plots reported by Nunan *et al.* (*31*), where the fresh catalyst exhibited a slow rise in conversion with temperature while the second run-up displayed the steeper gradient. However, as catalysts were aged in air/H$_2$O (*31*) as opposed to prereduction as used here, these differences are to be expected. Fresh Rh/Al$_2$O$_3$ catalysts under net-oxidising conditions were shown to exhibit multipeaked rate/

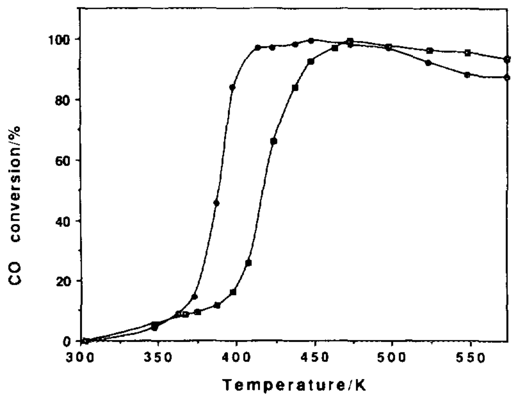

FIG. 7. Light-off curves for fresh (■) and rereduced (●) Pt-Rh(sim) catalysts heated at 10 K min^{-1} in CO(1%)/O$_2$(16%).

temperature plots (*7*) consistent with the behaviour of Rh(100) (*33*). Rereduced Rh/Al_2O_3 catalysts (*7*) and Rh(111) (*33*) do not display this phenomenon. Although Pt–Rh(100) is known to produce multipeak rate/temperature plots (*17*), this was not apparent here [Fig. 7]. This may indicate that following the initial reduction, the platinum–rhodium catalysts are in a more "metallic-state" (*32*) (i.e., lower dispersion) than for the monometallic component catalysts, exposing more {111}-type planes, and resulting in steeper light-offs. Consistent with this proposal, a previous study reports that Pt–Rh catalysts contained particles of a considerably greater particle size than those present in the monometallic catalyst (*34*).

Shift in ν(CO) during Catalytic Reaction

To obtain information regarding the nature of the metal particle composition, the frequency of the linear carbonyl species was followed as a function of temperature during reaction. Reaction between CO and oxygen over an initially CO-covered platinum surface takes place at the boundary between the adsorbed phases (*26*). This reaction between islands of CO and O gives rise to invariance in the frequency of the linear carbonyl band during reaction (*2–6, 35*) whereas reaction on an initially oxygen-covered platinum surface results in a constant shift of ν(CO) due to reaction occurring within a mixed CO/O ad-layer (*35*). Results for experiments conducted in a 1 : 16 CO/O_2 flow are shown in Fig. 8. As shown in previous studies for Pt/Al_2O_3 under nonisothermal conditions (*6, 8*), the carbonyl band frequency shows an initial decrease in frequency followed by a period of invariance before elimination of the species at a temperature above which 100% CO conversion in the stream occurs. As concluded previously (*8*), the actual frequency and the range of conversion during which invariance occurs will be determined by the size of the CO island created, and hence will be directed by the heterogeneity of the particle surface. The fresh Pt/Al_2O_3 sample [Fig. 8] shows invariance at 2064 cm^{-1} and during a temperature range equivalent to 80 to 100% CO conversion (*6*). In contrast, invariance at 2076 cm^{-1} for the rereduced catalyst extends over the conversion range of 10 to 100% (*8*). For rhodium, the linear carbonyl maximum shows a continual decrease in frequency, consis-

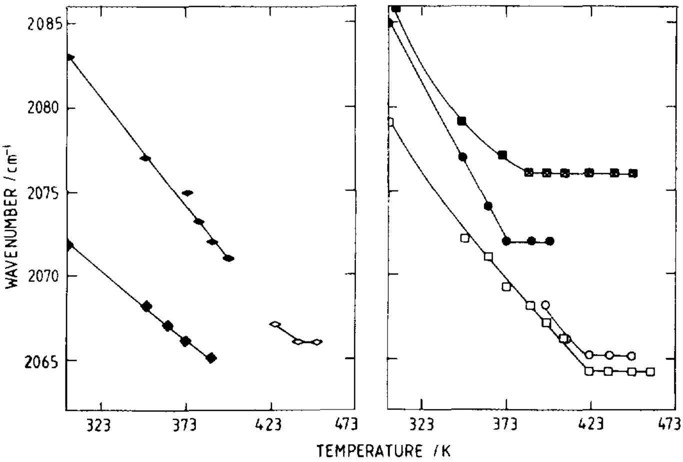

FIG. 8. Frequency (cm^{-1}) of the linear carbonyl band as a function of temperature while heating in CO(1%)/O_2(16%) for fresh catalysts (unfilled symbols) and rereduced catalysts (filled symbols) for Pt–Rh(step) (○, ●), Pt–Rh(sim) (◇, ◆), Pt/Al_2O_3 (□, ■), and Rh/Al_2O_3 (◇, ◆).

tent with previous reports (*7*, *9*) and indicative that reaction is occurring within a well mixed CO/O_2 adlayer.

When considering the fresh Pt–Rh catalysts, both samples displayed evidence of invariance in the carbonyl stretching frequency during heating in the 1 : 16 CO/O_2 mixture. Unlike the case of platinum alone (*6*) no correlation between a fixed CO conversion temperature and the temperature at which the onset of invariance occurred, was found for the bimetallic catalysts (*36*). This is attributed to the fact that at high O_2/CO ratios, fixed percentage CO conversion temperatures above 50% were dictated by platinum activity whereas at low ratios rhodium was the metal component which mainly controlled the form of the light-off curve. The invariance at 2064/5 cm^{-1} shown in Fig. 8 was independent of the CO/O_2 ratio, as long as oxygen was in excess (*36*). Invariance at 2065 ± 1 cm^{-1} for fresh bimetallic catalysts and Pt would suggest that the bimetallic catalysts contained either Pt-only particles with a surface heterogeneity similar to that of the particles in the Pt catalyst, or that bimetallic particles contain ensembles of Pt atoms sufficiently large to support such behaviour. Consistent with the effect observed for Pt only, rereduction of the Pt–Rh(step) catalyst resulted in an increase in the frequency of the linear carbonyl species during the invariance period, indicating an increase in the size of the CO islands formed. The slightly lower frequency (2072 cm^{-1}) during invariance, when compared with Pt alone (2076 cm^{-1}), would suggest either that the platinum particles within the bimetallic catalyst were less annealed by the pretreatment procedure, or that growth of island size was restricted by a boundary of rhodium atoms in the case of bimetallic particles.

As shown in Fig. 8, the rereduced Pt–Rh(sim) catalyst shows no period of invariance, indicating that the reaction proceeds in a mixed CO–O adlayer. This would suggest that no sufficiently large ensembles of Pt atoms exist following the pretreatment carried out. It is not likely that this results from a covering of the particle surface by rhodium atoms since by comparing the plot for rhodium with that of Pt–Rh(sim), the carbonyl stretching frequency lies somewhat above that of rhodium, suggesting a contribution from platinum carbonyls. Previous studies show that the linear carbonyl band frequency for Pt–Rh catalysts lies between those of the monometallic components (*18*, *23*, *34*). It is more likely, therefore, that the Pt–Rh particles contain a mixed metal surface which leads to formation of the mixed CO–O adlayer. It has been suggested (*17*) that such a mixing of CO and O on an alloy surface may result in a faster reaction at a lower temperature. However, as in that particular study and as shown here in Fig. 6, only marginal differences were observed between the Pt–Rh(sim) and (step) catalysts following rereduction despite differences in the manner in which the reaction proceeds.

Nature of the Exposed Metal

Results here indicate that modification of the Pt–Rh catalysts occurs in the presence of the reactant gas mixture which, under certain operating conditions, leads to an increase in catalytic activity. Such a phenomenon has been described for the oxidation of methane over Pd/Al_2O_3 and attributed to a decrease in metal dispersion (*37*) and to a restructuring of the metal surface (*37*, *38*). The latter process has been shown by infrared spectroscopy to occur for Pd/Al_2O_3 catalysts in the presence of CO (*39*).

As shown in previous studies of supported rhodium catalysts (*7*, *18*, *21–23*), heating in CO at 573 K is expected to reduce rhodium dispersion as a result of an agglomeration of the gem-dicarbonyl sites and the formation of rhodium particles with linear carbonyl adsorption sites. This may occur by two processes. In the first, heating in CO incorporates the dicarbonyl-site rhodium atoms into an existing cluster, increasing its size, and in the second a number of dicarbonyl site rhodium atoms come together to form small metal clusters (*7, 22*). From the form of the plots in Fig. 2, it would appear that during heating in CO, the original gem-dicarbonyl site atoms become incorporated into Pt or Pt–Rh particles, resulting in a much more rhodium-like behaviour of the carbonyl species. Although Fig. 2 shows only the frequency vs temperature plot for the Pt–Rh(step) catalyst, the Pt–Rh(sim) catalyst showed similar behaviour.

The question remains therefore that it rhodium incorporation into existing particles occurs during heating in CO for both samples, what is the reason for the differences in behaviour apparent for the CO oxidation process for the two 573 K CO-pretreated samples? The reason may lie in the differences between the original prepared samples. As indicated in the description of catalyst characterisation, TPR profiles for the two samples show certain similarities but also certain differences (*12*). Reduction maxima at 413 K [Pt–Rh(sim)] and at 418 K [Pt–Rh(step)], are consistent with a single maximum at 415 K for Pt–Rh/Al_2O_3, indicative of the reduction of Pt and Rh in close proximity, i.e., bimetallic particles (*40*). The main difference between the samples is the absence of a higher temperature peak for Pt–Rh(sim), which is apparent for both Pt–Rh(step) and for Pt alone. This would suggest that coimpregnation of the metal salts produces a catalyst with few platinum-only particles, while sequential impregnation produces platinum-only and platinum-rhodium particles (and probably rhodium-only particles in both cases). Heat treatment in CO at 573 K for Pt–Rh(sim) catalyst probably results in further rhodium incorporation into the existing Pt–Rh particles and possibly a redistribution of Rh atoms within the particle with a loss of the Pt ensembles and subsequently a loss in the invariance phenomenon exhibited by the fresh sample.

Low temperature IR studies of Pt–Rh catalysts prepared by coimpregnation show dipole coupling effects indicating the presence of particles exposing both metals in close proximity at the surface (*23*). Consistent with the presence of both types of metal particle, the initially reduced Pt–Rh (step) catalyst exposes both metals at the surface, as shown by the frequency of the bands due to bridged and linear bound carbonyls which lay between those values for the individual metals. Following heat treatment in CO above 508 K, Rh atoms are probably incorporated only into the peripheries of the platinum particles, thus leaving suitably sized Pt ensembles to produce the CO islands required to display the invariance phenomenon in the carbonyl stretching frequency. It is known that heating above 773 K in hydrogen is required to form a homogeneous Pt–Rh alloy particle (*41*) and hence the subsequent rereduction in H_2/Ar at 573 K is not expected to affect further the distribution of atoms within the particles.

CONCLUSIONS

Several temperature run-ups in CO/O_2 may be required to give a Pt–Rh catalyst displaying stable activity. Heating the fresh catalyst under CO-rich conditions leads to decreased light-off temperatures for subsequent run-ups due to a decrease in rhodium dispersion induced by agglomeration of the gem-dicarbonyl adsorption sites. The nature of the surface composition following incorporation of these rhodium atoms into existing particles may be deduced from the manner in which the linear carbonyl frequency changes during reaction. Well-mixed CO/O adlayers as indicated by continual frequency changes did not lead to improved catalyst performance relative to catalysts with surfaces that exhibited evidence for CO islands as identified by invariance in the carbonyl frequency.

ACKNOWLEDGMENTS

I thank Johnson Matthey for the loan of a rhodium nitrate sample and for access to the TPR facility. My thanks go to Miss H. Shaw for her assistance in connection with the latter. XPS analysis was carried out by Mr. B. Williams, Leverhulme Centre for Innovative Catalysis, University of Liverpool, to whom I am most grateful.

REFERENCES

1. Taylor, K. C., *in* "Catalysis—Science and Technology" (J. R. Anderson and M. Boudart, Eds.), Vol. 5, p. 120. Springer-Verlag, Berlin, 1984.
2. Cant, N. W., and Donaldson, R. W., *J. Catal.* **71,** 320 (1981).
3. Barshad, Y., Zhou, X., and Gulari, E., *J. Catal.* **94,** 128 (1984).
4. Haaland, D. M., and Williams, F. L., *J. Catal.* **76,** 450 (1982).
5. Li, Y-E., Boecker, D., and Gonzalez, R. D., *J. Catal.* **110,** 319 (1988).
6. Anderson, J. A., *J. Chem. Soc. Faraday Trans.* **88,** 1197 (1992).
7. Anderson, J. A., *J. Chem. Soc. Faraday Trans.* **87,** 3907 (1991).
8. Anderson, J. A., *Catal. Lett.* **13,** 363 (1992).
9. Li, Y-E., and Gonzalez, R. D., *J. Phys. Chem.* **92,** 1589 (1988).
10. Kiss, J. T., and Gonzalez, R. D., *J. Phys. Chem.* **88,** 898 (1984).
11. Anderson, J. A., and Rochester, C. H., *Catal. Today* **10,** 275 (1991).
12. Anderson, J. A., and Williams, B., *in* "Catalysis and Surface Characterisation" (T. J. Dines, C. H. Rochester, and J. Thomson, Eds.), p. 136. Royal Society of Chemistry, London, 1992.
13. Cooper, B. J., Harrison, B., Shutt, E., and Lichtenstein, I., Amer. Chem. Soc., Society of Automotive Engineers Technical Paper Series, Paper 770367 (1977).
14. Oh, S. H., and Carpenter, J., *J. Catal.* **98,** 178 (1986).
15. Powell, B. R., and Chen, Y-L., *Appl. Catal.* **53,** 233 (1989).
16. Kim, S., and D'Aniello, M. J., *Appl. Catal.* **56,** 45 (1989).
17. Siera, J., van Silfhout, R., Rutten, R., and Nieuwenhuys, B. E., *in* "Proc. 2nd Int. Sym. Catal. and Aut. Poll. Cont. CaPoC 2" (A. Crucq, Ed.), *Stud. Surf. Sci. Catal.*, Vol. 71. Elsevier, Amsterdam, 1991.
18. Anderson, J. A., and Rochester, C. H., *J. Chem. Soc. Faraday Trans.* **87,** 1479 (1991).
19. Yang, A. C., and Garland, C. W., *J. Phys. Chem.* **61,** 1504 (1957).
20. Yates, J. T., Jr., Duncan, T. M., and Vaughan, R. W., *J. Chem. Phys.* **71,** 3908 (1979).
21. Solymosi, F., and Pásztor, M., *J. Phys. Chem.* **89,** 4789 (1985).
22. Dictor, R., and Roberts, S., *J. Phys. Chem.* **93,** 2526 (1989).
23. Anderson, J. A., and Solymosi, F., *J. Chem. Soc. Faraday Trans.* **87,** 3435 (1991).
24. Wang, T., and Schmidt, L. D., *J. Catal.* **70,** 187 (1981).
25. Peri, J. B., *J. Catal.* **52,** 144 (1978).
26. Engel, T., and Ertl, G., *in* "Advances in Catalysis" (D. D. Eley, H. Pines, and P. B. Weisz, Eds.), Vol. 28, p. 2. Academic Press, New York, 1979.
27. Sant, R., and Wolf, E. E., *Chem. Eng. Sci.* **45,** 3137 (1990).
28. D'Aniello, M. J., Monroe, D. R., Carr, C. J., and Krueger, M. H., *J. Catal.* **109,** 407 (1988).
29. Bosch-Driebergen, A. G., Kieboom, M. N. H., Dreumel, A., Wolf, R. M., Delft, F. C. M. J. M., and Nieuwenhuys, B. E., *Catal. Lett.* **2,** 73 (1989).
30. Nunan, J. G., Robota, H. J., Cohn, M. J., and Bradley, S. A., *J. Catal.* **133,** 309 (1992).
31. Nunan, J. G., Cohn, M. J., and Donner, J. T., *Catal. Today* **14,** 277 (1992).
32. Yao, Y-F. Y. *J. Catal.* **87,** 152 (1984).
33. Schwartz, S. B., Schmidt, L. D., and Fisher, G. B., *J. Phys. Chem.* **90,** 6200 (1986).
34. van Slooten, R. F., and Nieuwenhuys, B. E., *J. Catal.* **122,** 429 (1990).
35. Shigeishi, R. A., and King, D. A., *Surf. Sci.* **75,** L397 (1978).
36. Anderson, J. A., unpublished results.
37. Briot, P., and Primet, M., *Appl. Catal.* **68,** 301 (1991).
38. Baldwin, T. R., and Burch, R., *Appl. Catal.* **66,** 337 (1990).
39. Hicks, R. F., Haihua, Q., Kooh, A. B., and Fischell, L. B., *J. Catal.* **124,** 488 (1990).
40. Martens, J. H. A., and Prins, R., *Appl. Catal.* **46,** 31 (1989).
41. Wang, T., and Schmidt, L. D., *J. Catal.* **71,** 411 (1981).